IMPLEMENTATION OF A FLIGHT SIMULATION TOOL INTO A ROTORCRAFT DESIGN ENVIRONMENT

Michel Buchwald, michel.buchwald@dlr.de, DLR Institute of Flight Systems, Germany
Peter Weiand, peter.weiand@dlr.de, DLR Institute of Flight Systems, Germany
Dominik Schwinn, dominik.schwinn@dlr.de, DLR Institute of Structures and Design, Germany
Florian Wolters, florian.wolters@dlr.de, DLR Institute of Propulsion Technology, Germany

Abstract

The German Aerospace Center (DLR) is currently developing a new integrated design environment called IRIS (Integrated Rotorcraft Initial Sizing). This framework features distributed computation on the servers at different locations using the DLR collaboration software RCE (Remote Component Environment) and the data model CPACS (Common Parametric Aircraft Configuration Schema). The flight performance calculation is one of the main parts within a sizing loop. To compute and analyze the flight mechanic properties the simulation tool HOST (Helicopter Overall Simulation Tool) developed by Airbus was integrated into the process. The purpose of this paper is to provide an overview of the rotorcraft design environment IRIS and the necessary calculations before using a flight performance calculation. Afterwards the implementation of such a complex flight performance calculation tool into the design environment IRIS involving the automatization of the pre- and post-processing procedures will be described. For mission performance calculation, a physics based engine model is integrated and coupled with the trim and performance calculation conducted by HOST. The presented results are considering different requirements like main rotor geometries or mission specifications. Beyond sizing and mission analysis the same tools are used to compute load cases in order to deliver the necessary input for a more sophisticated structural analysis and design.

Keywords

Rotorcraft design; flight performance; conceptual and preliminary design; fuel estimation; high velocity configurations

NOTATIONS

Symbols

c_{MR}	Main rotor chord, m
$C_{l\alpha}$	Lift curve slope, 1/rad
e_β	Normalized radius of flapping hinge, -
J_β	Blade mass moment of inertia about the flapping moment, kg m
m_{BEM}	Basic empty mass, kg
m_{blade}	Blade mass, kg
$m_{bl,\beta}$	Dynamic blade mass, kg
m_F	Fuel mass, kg
m_{MTOM}	Maximum take-off mass, kg
n_x, n_y, n_z	Load factors along all three axis, -
N_b	Number of blades, -
P_{ideal}	Ideal power, W
P_{inst}	Installed power, W
P_{MCP}	Maximum continuous power, W
P_{OEI}	Power one engine inoperative, W
P_{TO}	Power take-off, W
R_{MR}	Main rotor radius, m
V_h	Horizontal velocity, m/s
$V_{h_{new}}$	Reduced horizontal velocity, m/s
$x_{CG,bl}$	Center of gravity for dynamic blade mass, -
σ	Rotor density, -
Ω_{MR}	Rotor speed, rad/s
γ	Lock number, -
ρ	Density, $kg\,m^{-3}$
$\mu_{CG,bl}$	Center of gravity of the beam element, -
$\mu_{m,bl}$	Blade tip mass ratio, -

Abbreviations

ACT/FHS	Advanced Control Technology / Flying Helicopter Simulator
ADS	Aeronautical Design Standards
AFDD	U.S. Army Aeroflightdynamics Directorate
CAMRAD II	Comprehensive Analytical Model of Rotorcraft Aerodynamics and Dynamics
CPACS	Common Parametric Aircraft Configuration Schema
C.R.E.A.T.I.O.N	Concepts of Rotorcraft Enhanced Assessment Through Integrated Optimization Network
DLR	German Aerospace Center (Deutsches Zentrum für Luft- und Raumfahrt)
EDEN	Evaluation and Design of Novel Rotorcraft Concepts
HOST	Helicopter Overall Simulation Tool
IRIS	Integrated Rotorcraft Initial Sizing
ISA	International Standard Atmosphere
MCP	Maximum Continuous Power
MDO	Multidisciplinary Design and Optimization
NDARC	NASA Design and Analysis of Rotorcraft
OEI	One Engine Inoperative
RCE	Remote Component Environment
RIDE	Rotorcraft Integrated Design and Evaluation
TLAR	Top Level Aircraft Requirement
TO	Take-off
TRIAD	Technologies for Rotorcraft in Integrated and Advanced Design

1. INTRODUCTION

1.1. Motivation

Disciplines like aerodynamics, structural design, engine performance and flight performance calculation are involved to develop rotorcraft configurations turning rotorcraft design into a highly multidisciplinary and one of the most complex design challenges in aerospace engineering.

Currently the German Aerospace Center (DLR) is developing a new design environment for rotorcraft [1]. These activities started in 2010 with the first internal project RIDE (Rotorcraft Integrated Design and Evaluation) and followed in 2014 by the project EDEN (Evaluation and Design of Novel Rotorcraft Concepts) focusing on creating a tool chain for rotorcraft design. These initial projects were a collaboration of the DLR Institutes of Flight Systems, Aerodynamic and Flow Technology, and Structures and Design. In 2018 the current project TRIAD (Technologies for Rotorcraft in Integrated and Advanced Design) started. The goal of this project is to predict the impact of new technologies, such as wing combinations, additional thrust generators or composite materials on a virtual rotorcraft and new high speed configurations. This implies an extension of the existing tools and build-up of the new rotorcraft design environment IRIS (Integrated Rotorcraft Initial Sizing). With project TRIAD the collaboration of the three initial institutes is extended by the Institute of System Architectures in Aeronautics and the Institute of Aerospace Medicine.

1.2. Rotorcraft design process

The general design process of a rotary-wing aircraft is similar to fixed-wing design and can be divided into three main phases (see FIG 1) according to Raymer [2]. After defining the Top Level Aircraft Requirements (TLARs) and the technical state of the art the conceptual design phase can be carried out. The required results of the first phase are the dimensions of the external configuration, a mass and balance estimation, and a first flight performance calculation for the design case as well as the analysis of some off-design cases. With the decisions and results of the first phase almost 65% of the expected life cycle costs are defined according to Roskam [3]. The second design phase is called preliminary design. To finalize the exact shape of the external configuration more extensive tasks are required, for example definition of the basic internal arrangement, solve all flow problems, conduct an extended flight performance computation and compute the major load cases need to be conducted. Reliable cost estimation can also be part of the preliminary design since the impact on the life cycle costs rises up to 85% by completing the second phase. The third and last design phase before starting the manufacturing process is the detailed design phase. This is the most complex phase requiring an enormous amount of personnel. In this last phase the focus is on designing the mechanisms, tooling and the manufacturing process, including the production of a prototype for flight tests.

To deliver solutions for the conceptual phase of design research institutes developed design tools for the

rotorcraft. For example ONERA developed C.R.E.A.T.I.O.N [4] [5] which is a multidisciplinary computation platform for the evaluation of rotorcraft concepts with respect to environmental impact and flight performance. NASA developed NDARC (NASA Design and Analysis of Rotorcraft) [6] which is an analysis tool for rotorcraft systems. For comprehensive analysis beyond mission performance the sizing results are extracted to CAMRAD II (Comprehensive Analytical Model of Rotorcraft Aerodynamics and Dynamics) [7].

The objective of the DLR design environment IRIS is to cover the conceptual and parts of the preliminary design. Detailed design for production is not part of these activities. To perform a scientific case study in terms of conceptual and partly preliminary design, the trim and flight performance calculation is one of the most important features of rotorcraft design. Here DLR follows a very specific approach by integrating the Airbus developed simulation tool HOST (Helicopter Overall Simulation Tool) into IRIS. HOST is used to conduct the mission related performance computation inside the primary sizing loop, where the basic empty and fuel mass are iteratively computed. Consequently the results of the flight performance calculation directly affect the dimensions of the virtual configuration during sizing.
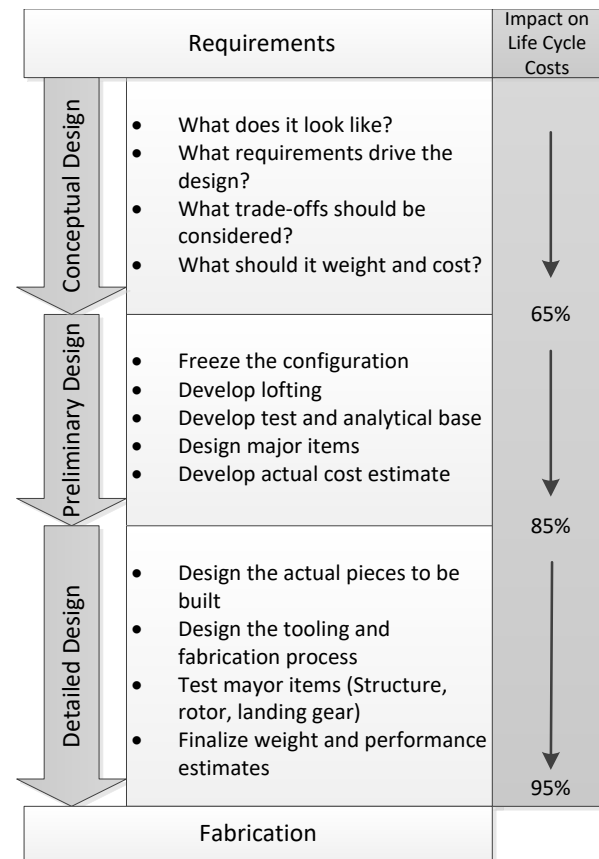

FIG 1   The three phases of aircraft design

Therefore the generation of the flight simulation model including the parametrization of its components has to be on a high level of reliability since the dimensions of the virtual configuration are changing during the overall process.

This paper will provide an overview of the rotorcraft design environment IRIS and the implementation of the high fidelity flight simulation tool HOST into it, involving the automatization of the pre- and post-processing procedures. The possibility to compute performance requirements, like load cases after a converged sizing, with the same code and therefore with the same accuracy as the mission requirements during sizing is a beneficial feature in order to minimize uncertainties.

1.3. Tool Level

The tools used during an aircraft design process have a wide span of physical basis. The set of results and the computation time also differ. To compare the different tools according to their physical modelling levels a classification in four levels ranging from 0 to 3 is made. ONERA shows a similar tool classification [8]. In FIG 2 the four tool levels based on their computation time and required input data versus the resulting uncertainties und the robustness are shown.
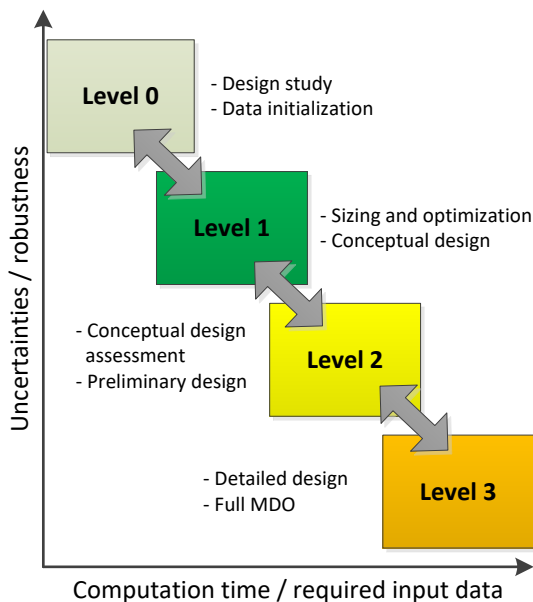

FIG 2   Tool level classification

After defining the top level aircraft requirements (TLARs) for a new case study the overall process starts with the Level 0 tools. These tools have a low computation time and do not need much input data and therefore are used for a first data initialization based on statistics and simple mathematical equations. In contrast to the computation time, the uncertainties and the robustness is the highest at Level 0 tools (see FIG 2). The tools for conceptual design and optimization using higher iterative procedures are classified as Level 1 tools. For instance, codes applying the blade element theory are classified as Level 1 tools. For the procedures of the comprehensive analysis of a conceptual design study as well as the preliminary design the tools used are classified as Level 2. An example for Level 2 tools is the unsteady panel method coupled with a free-wake code. These computations are arranged without performing an automated recursive loop. Tools with the lowest uncertainties and robustness are classified as

Level 3. These tools cover the latest parts of preliminary design and the detailed design including numerical methods like CFD and full MDO (Multidisciplinary Design and Optimization) calculations. Thereby the computation time and the required input data are the highest of all tools. HOST can be defined as a Level 1 tool using trim calculation or Level 2 tool for complex time simulation.

A particular feature of IRIS is the combination of Level 0 and Level 1 tools by a universal data model. This allows the step back and repetition of the conceptual design based on the Level 2 results.

2. INTEGRATED ROTORCRAFT INITIAL SIZING

2.1. Collaboration and data model

The primary element of the design environment IRIS is the primary sizing loop, which is build up with the collaboration software RCE (Remote Component Environment) [9]. This open-source software is developed by the DLR [10]. RCE allows distributed calculation on different servers located at different facilities. On one hand the tools remain on the server of the responsible institutes for maintenance and administration. On the other hand it is still possible to develop and set up the iterative procedures to perform a sizing task and provide access for all partners without entering the code.

In order to save and manage all important parameters generated during a sizing process a sophisticated interface is needed. Following the experience from fixed-wing projects, the DLR developed data model CPACS (Common Parametric Aircraft Configuration Schema) [11] was harmonized with the design environment for rotorcraft. This XML data model was developed to store all necessary information in one file that is accessed by every tool. The principle of one central data model is shown in FIG 3.
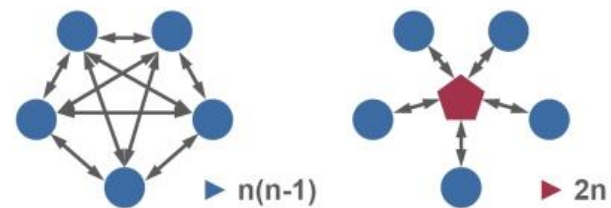

FIG 3   Principle functionality of a conventional interface (left) and the CPACS data model (right)

The left side of FIG 3 shows a conventional approach with a high number of interfaces. The right side shows the concept of the universal data model that allows a central storage of data during the process. To use CPACS in IRIS it was necessary to extend the data model with a new rotorcraft path to describe a virtual rotorcraft configuration. This new path is now part of the official CPACS version but is still under strong development during the actual project. With the rotorcraft add-on CPACS become the universal input and output format for every tool in the design environment. This enables the possibility to quickly rearrange workflows in the graphical user interface of RCE and integrate new tools.

2.2. Conceptual Sizing

The sizing workflow considered for IRIS is arranged in different phases (see FIG 4). The overall process starts with the initialization of the first configuration (Level 0). The next step is the primary sizing loop (Level 1). This approach is very conventional by iterating the maximum take-off mass. In this paper particular attention is paid on the flight performance computation for the mission specific fuel mass inside the primary sizing loop. The resulting configuration shows its external dimensions, its masses and its required flight performance in a balance. This state of results is considered as a consistent design.
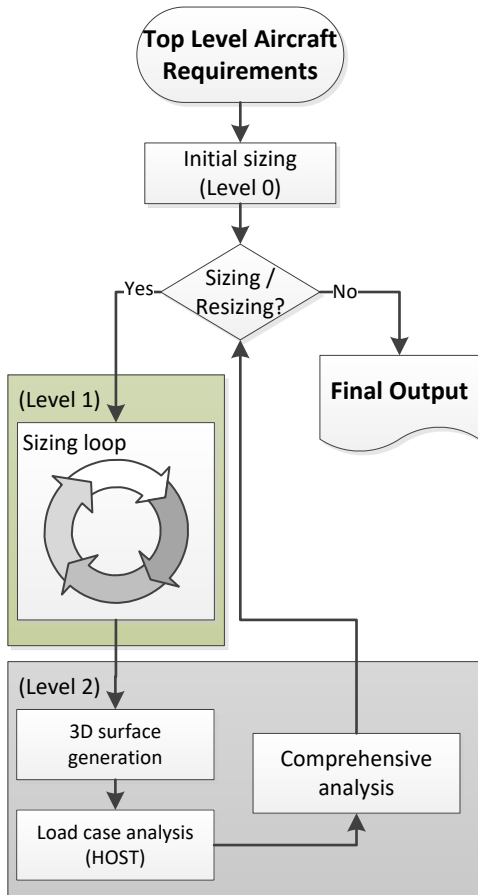

FIG 4   IRIS workflow

In present case of the design environment IRIS the trim and performance calculation in the primary sizing loop as well as in the following load case analysis is conducted with HOST. A typical source for uncertainties by switching from one computational code to another can be excluded. On the other hand the early implementation of HOST will require some special considerations.

On basis of a consistent design the comprehensive analysis including higher fidelity tools is performed (Level 2). The latter part will be discussed briefly in section 2.3.

2.2.1   Initialization of the first data

Starting from the beginning involves a careful consideration of the mission, performance and technical requirements. The mission requirements describe the design case and usage of the new vehicle. Here in principle its mission profile has to be defined. The performance requirements describe several off-design points besides of the design mission. The technical requirements specify the characteristics of the configuration, like arrangement of rotors, stabilizers, wings and further more different sorts of components.

The minimum parameters necessary to initialize the first configuration are listed in TAB 1. Besides the minimum these parameters include some optional requirements in order to improve and supply the configuration.

TAB 1   Minimum and optional TLARs for intitialization

Minimum Parameter	Unit
Payload mass	kg
Cruise speed	m/s
Range	km
Number of main rotor blades	-
Main rotor arrangement	-
Optional Parameter	
Blade geometry (Main/Tail rotor)	-
Mission profile	-
Inner dimensions of the middle fuselage section (height/width/length)	m
Cargo hold payload fraction	-
Design blade loading	-
Design disk loading	N/m²
Reference rotor radius	m
Reference altitude	m
Reference air temperature	°C

The methods applied cover empirical and simple physical equations. As shown in FIG 2 this procedures are very fast featuring the highest robustness and the highest uncertainties. The amount of data computed with the level 0 tools must be sufficient to start the iterative sizing procedure described in the following sections.

2.2.2   Sizing task

The fundamental function of this procedure is to deliver sizing rules that describe and scale the external configuration of the rotorcraft as a function of the maximum take-off mass by taking into account defined reference conditions. The conditions considered here are typically used to size the lifting components and are related to hover or cruise flight. A typical condition for instance is a required hover blade loading with maximum take-off mass at certain altitude and air temperature.

The derivation of the external configuration requires a parametrization of the individual components of the rotorcraft. This includes dimensions, translations and orientations of rotors, fuselage, wings and stabilizers. In the first step the dimensions of the rotors are determined by computing the radius and the solidity:

$$(1) \qquad \sigma = \frac{N_b \, c_{MR}}{(\pi \, R_{MR})}$$

Lifting surfaces, no matter whether wing or stabilizer, are defined by their segments, which means at least one segment is required with a root and a tip section and are scaled by their reference area. The dimensions of the fuselage are determined by starting in the shape of the cross section of the cabin and extracting the mid part. Sections for cockpit and tail cone are added to form the fuselage body. The length of the tail boom is derived from the position of the most rear mounted components like stabilizers, anti-torque devices, and propellers. The individual components for the assembly are shown in FIG 5.
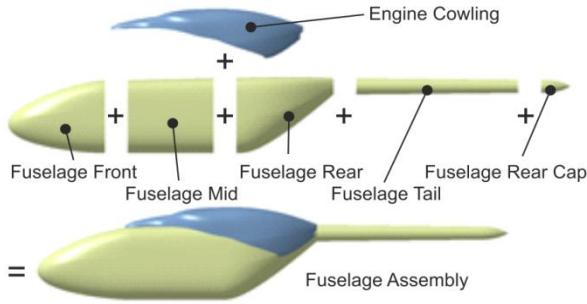

FIG 5   Scaleable components used to assembly a generic fuselage

The shape of the parts can be adapted to different arbitrary templates depicting existing configurations or creating new ones. The individual components of the rotorcraft are placed in relation to the determined center of gravity for reasonable flight mechanic properties. The exact position and orientation is given by individual scripts for every specific configuration. Here the arrangement of rotors, wings and stabilizers is controlled by geometric equations. Not only different configurations like main/tail rotor or coaxial rotors configurations are defined; also adaption of one configuration to different versions is possible. For instance a cross tail with the tail rotor on the same height like the main rotor and a lower horizontal stabilizer can be adapted to a T-tail with the tail rotor at the root of the vertical stabilizer and in line with the tail boom. A none-dimensional description of the component positions is extremely sensible due to the possibility of feeding back results from comprehensive analysis and higher fidelity tools. A simple update of parameters ensures a reliable resizing of the virtual configuration.

2.2.3   Rotor blade sizing

There is a wide variety of blades available for rotorcraft depending on the requirements for the overall configuration and mission performance. The solution of this step must be to get a definition of the rotor that is suited for a blade element method computation. From the requirements the desired blade geometry as well as the number of blades is available (see TAB 1). After the sizing of the external configuration the rotor radius and solidity are available as well. The combination of solidity and number of blades results in the mean chord of one blade allows the scaling of the abstract ratio of a reference blade to the desired planform. A choice of several reference blades is available in a data pool:

- Rectangle blade (similar to BO105)

- Rounded tip blade (similar to EC135)
- 7AD
- ERATO [12]

This list is unlimited to expand. The coordinates are normalized along the radius (from 0 to 1) including all airfoil section with their corresponding chord, sweep and angle of incidence.

Even for a pure flight performance computation the aerodynamic properties need to be associated with the simple one per revolution harmonic oscillation of the blade. Most reasonable parameter to cover aerodynamic and gyroscopic forces of a rotating blade is the Lock number (see equation (2)). Here in the numerator the aerodynamics are represented by air density, chord length, radius and equivalent 2D lift gradient. The second moment of inertia for flapping motion is given in the denominator.

(2)
$$\gamma = \frac{\rho \, c_{MR} \, R_{MR}^4 \, C_{L\alpha}}{J_\beta}$$

For a required Lock number and a given blade planform the corresponding second moment of inertia can be calculated. A simple blade model consisting of a beam element from flapping hinge to the tip and a mass point at the tip delivers the dynamic mass for the trim calculation (see equation (3)). Here the ratio of the tip mass over the overall blade mass is given by $\mu_{m,bl}$. The normalized radius of the flapping hinge is given by e_β.

(3)
$$m_{bl,\beta} = J_\beta \left[\left(\frac{1 + 2 \, \mu_{m,bl}}{3} \right) \left[(1 - e_\beta) \, R_{MR} \right]^2 \right]^{-1}$$

The center of gravity of the beam element, and mass ratio between the point mass and the resulting dynamic mass are tuning factors to calibrate the model to a reliable reference blade by maintaining the scalability of the blade. Equation (4) delivers the location of the center of gravity for the dynamic blade mass on the radius. The relative position of the center of gravity of the beam element is given by $\mu_{CG,bl}$.

(4)
$$x_{CG,bl} = R_{MR} \left[(e_\beta + (1 - e_\beta) \, \mu_{CG,bl})(1 - \mu_{m,bl}) + \mu_{m,bl} \right]$$

2.2.4   Calculation of the aerodynamic properties

Acquiring reliable tables for the aerodynamic coefficients depending on angle of attack and angle of side-slip is still a problematic procedure and source for errors. For the fuselage forces and moments along and around three axes are required. For stabilizers tangential and normal force, as well as the longitudinal moment is the minimum. For wings the side force may be neglected. When using larger wings with high aspect ratio the yaw-roll and yaw-yaw moments must not be neglected.

The conventional computation method would be using a CFD tool like the DLR TAU code [13]. The pre-processing, computation and post-processing time is at maximum and cannot be performed without great user interference.

An alternative is the computation with a panel code. Here the possibility of deriving the geometry from the CPACS file and build a surface mesh without guidance by the user is possible [14]. Here it is possible to compute the coefficients for the clean surface and later add the additional components, like rotor hub, landing gear, winch and so on. The drag areas of these components are calculated by handbook methods. For an example of a parametric estimation of the hub drag see [15]. These additional sources of drag for the individual components are placed on the location of impact on the fuselage taking into account the offset to the aerodynamic reference point and the influence not only on the forces, also on the moments. Panel codes are applying potential theory. In the present case a calculation of the boundary layer is integrated in order to compute viscous drag besides of pressure drag. This includes an estimation of the separation line with a prediction of the pressure behind this line. Until now this approach exhibited limited reliability. For configurations showing a long tail cone and a small or even no separation computation showed good agreement with higher fidelity or wind tunnel results. For configurations showing a blunt tail cone with larger area of separation the coefficients showed irregular errors. Hence results have to be checked for correctness what forbids the use inside a loop.

Therefore aerodynamic coefficients must be computed before iterating the maximum take-off mass. Inside the sizing loop a scaling of the reference area is applied.

2.2.5 Estimation of Installed power

In order to find a sensible installed power for a given maximum take-off mass and rotor disc area the factor of the installed power ratio was introduced. This factor is the ratio of the installed power over the ideal power in hover (out of ground effect) condition at sea level ISA (see equation (5)).

$$(5) \qquad \frac{P_{inst}}{P_{ideal}} = \frac{P_{inst}}{\sqrt{\dfrac{(m_{MTOM}\,g)^3}{2\,\rho\,\pi\,R_{MR}^2}}}$$

The ideal power is simply calculated by momentum theory from the weight force at maximum take-off mass as thrust and air density for ISA sea level.

First reliable values can be derived from statistics. FIG 6 shows the maximum installed power factor over the mission flight mass for some existing rotorcraft configurations. For transport helicopters the mission flight mass equals the maximum take-off mass. For attack helicopters it is less.

The investigation of a specific configuration can be difficult since some military models show different rating levels or the corresponding value is not available. In addition to FIG 6 the configuration with their installed engine models and the corresponding power factors for OEI (one engine inoperative), TO (take-off) and MCP (maximum continuous power) are listed in TAB 2.
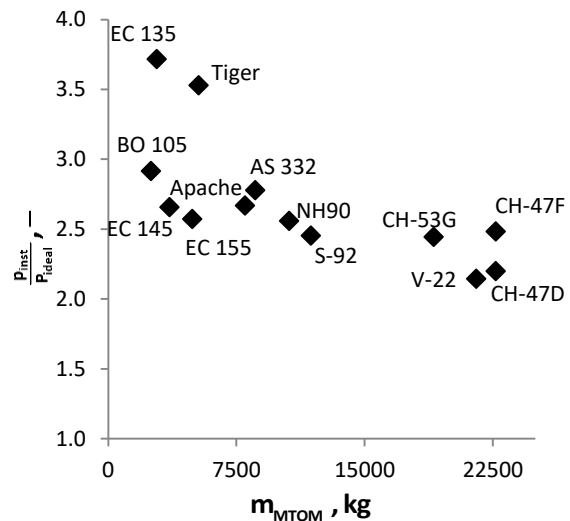

FIG 6 Installed power factor (maximum 30sec OEI rating) over maximum take-off mass for several existing configurations

For the CH-53E, the CH-53G and the NH90 the ratings for OEI are currently not available. The corresponding data in FIG 6 show the power factor with the take-off power (see TAB 2). Furthermore for the CH-47D, the CH-47F, the MD Apache and the Explorer, the factors for take-off power are not included in TAB 2. The power factors for the MCP ratings are a good reference for hot and high capabilities but are not sufficient to take emergency cases into account like in particular considered by the EC135 and the Tiger.

TAB 2 Different rotorcraft with their installed engines and the corresponding power factors for cases OEI, TO and MCP (data derieved from Jane's Helicopter Markets and Systems [16])

Rotorcraft	Engine	$\dfrac{P_{OEI}}{P_{ideal}}$	$\dfrac{P_{TO}}{P_{ideal}}$	$\dfrac{P_{MCP}}{P_{ideal}}$
CH-53E	T64-GE-416	/	1.75	1.48
CH-47D	T55-L-712SSB	2.20	/	1.60
CH-47F	T55-GA-714A	2.48	/	2.13
V-22	AE1107C	2.14	2.14	2.05
CH-53G	T64-GE-100	/	2.44	2.15
S-92	GE CT7-8A	2.45	2.26	1.83
NH90	RTM322	/	2.56	2.43
AS 332	Makila 1a2	2.78	2.43	2.18
Apache	T700-GE-701	2.67	/	2.60
Tiger	MTR 390	3.53	2.91	2.66
EC 155	Arriel 2c2	2.57	2.30	2.13
EC 145	Arriel 1E2	2.66	2.54	2.39
MDExplorer	PW207Es	2.84	/	2.38
EC 135	Arrius2B2	3.72	2.76	2.60
BO 105	Allison250-C20B	2.91	2.65	2.62

In general reasonable values can be found in the range of 2.4 up to 3 depending on the performance requirements. Higher requirements for emergency cases like OEI increase the value to more than 3.5.

The converged external configuration is the basis for a comprehensive analysis. Here very specific performance requirements can be analyzed by simulating very precise maneuvers. The results are needed to find ratings for the engine. Such complex simulation can be conducted with HOST, but not inside a sizing loop. However it is easy to update initial values for equation (5) based on statistics like shown in FIG 6 and TAB 2 and repeat sizing.

2.2.6   Sizing of the engine model

The initial model is based on the Turbomeca / Safran Helicopter Engines Arrius 2B2 engine, which is installed on the Eurocopter EC135 rotorcraft. Since the design cases presented in chapter 4 are a variation of the TLARs related to the EC135 it is consistent to relate the engine model to the Arrius 2B2.

A two spool turbo shaft performance model of the engine was created to provide sufficient performance data for the helicopter sizing process. The thermodynamic engine model represents a typical rotorcraft engine and is designed by means of DLR's in-house performance code GTlab performance [17].

Performance studies for both design and off-design conditions were conducted to fulfill dedicated engine power requirements at different flight conditions, e.g. like max power, continuous power and hovering.

For flight mission simulations the engine's performance was calculated throughout a typical flight envelope. The engine's performance data was stored for pre-selected parameters, like power, fuel flow, temperatures etc., in a data table, so-called performance map. However, the selection can be adjusted at any time. Since the performance requirements for the engine can also change during the design process of the rotorcraft, further engine designs were created, one representing an engine scaled by +20% and the other by -20% in air mass flow. The technology level was kept constant, but the mass flow effects in the component efficiencies were taken into account to consider non-linear effects on the engine characteristics. In addition, the spool speeds were adjusted accordingly. In order to enable an analysis under Hot Day requirements, further performance maps for the ISA +20K condition were created for all engine designs.

The performance maps saved in the CPACS file are later used to compute the fuel consumption depending on the required flight condition during the mission performance calculation (see section 3.3).

2.2.7   Analysis and estimation of maximum take-off mass

After scaling the external configuration including all its components as well as the installed power the analysis part of the primary sizing loop is performed in order to estimate the maximum take-off mass of the virtual configuration. Here the fundamental assumptions, in particular the fuel and basic empty mass, from the

initialization are recalculated and lead back to the sizing task (see section 2.2.2).

The fuel mass is calculated for a specific design mission. In case of IRIS the Airbus developed tool HOST was integrated to solve the trim and performance calculation. The details of these procedures are discussed in chapter 3.3.

The second part of the analysis is the estimation of the basic empty mass by computing all component masses. Several empirical models have been tested in the last years. In the recent applications the AFDD models presented by Johnson [6] are used. These models feature the largest number of input parameters and therefore the highest sensitivity to small design changes. All component mass equations need to be calibrated to the desired technological state of the art. This state takes the technical evolution as well as the scope of application into account. Besides the development time the type of helicopter is important. For instance even by considering the scalability of the models the calibration factors for a 3t helicopter for medical transport and a 10t transport helicopter are clearly not identical even for identical time of development.

2.3.   Analysis with higher fidelity tools

A consistent external configuration is the basis for applying higher fidelity tools as well as conducting a comprehensive analysis of the design case (see FIG 4). A comprehensive analysis typically includes extensive flight performance computation beyond the range of the design mission, sophisticated analysis of the performance requirements and assessment of stability.

The possibility to simulate the full maneuver envelope introduces the possibility for a more sophisticated structural analysis at a comparably early time point in the design process. Performance requirements not only include aerodynamic and flight mechanical considerations but also structural demands.

To save structural properties similar to the 3D geometry inside the CPACS data model is also possible. The principle of different structural arrangements analyzed on a given geometry is shown in FIG 7. The approach uses a finite element modelling to analyze and size the primary structure of the rotorcraft. More details of the process are described in [18]. To provide qualitative and quantitative sufficient input the possibility to compute an unlimited list of load cases must be developed. Since the maneuvers under consideration may be complex the computation is performed with the integrated HOST and described in section 3.6.
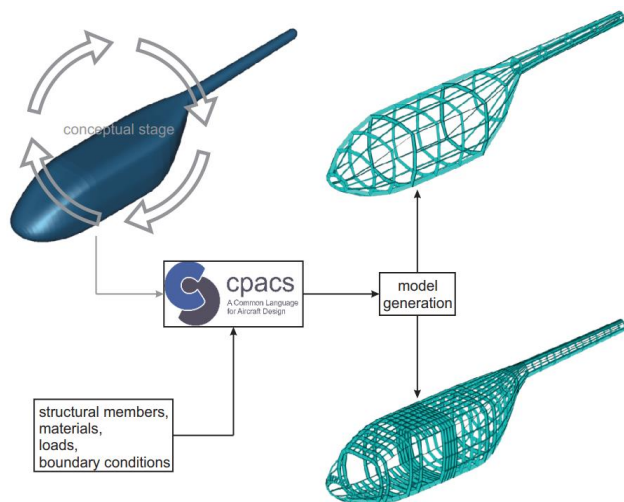
FIG 7   Schematic diagram of structural modelling using CPACS as data model and tool interface

3.   FLIGHT PERFORMANCE ANALYSIS

3.1.   Helicopter Overall Simulation Tool

HOST was developed by Airbus during the 1990s. The tool comprises the R85 code, which was developed for rigid and elastic blade simulations, and the helicopter simulation code S80 [19]. HOST offers three main functions. Trim calculation, time domain simulation and equivalent linear systems. Currently IRIS uses the blade element theory based trim calculation for flight performance calculation and thereby the Meijer-Drees induced velocity model. During the sizing loop HOST is executed in batch mode to estimate the fuel mass in combination with a scalable engine model. The procedures of pre-processing, execution and post-processing have to work automatically without user guidance.

3.2.   Preprocessing and model generation

The major part of the pre-processing is the generation of the flight mechanic model. Therefore all necessary data need to be extracted from the CPACS XML-file to build the several models. A series of python and shell scripts is used to write the data correctly into all the required module files. The following modules have to be generated at least [20]:

- Rotors (main rotor, anti-torque and propellers)
- Blades (main rotor, anti-torque and propellers)
- Aerodynamics of components (fuselage, wings, stabilizer)
- Cell
- Swashplate
- Engine

HOST enables a wide spectrum of implement different components to model a rotorcraft in more detail, but to get first results a basic model like described previously is sufficient. The rotor files of main rotor, anti-torque or propeller contain general information, e.g. the positioning, number of blades, mean chord, rotating speed. To describe the thrust generators in detail also the blade geometry in detail with chord, twist, mass, inertia and airfoil for every section have to be defined. Hub geometry with positions of prelead/lag, precone, lead/lag, flapping pitch and parameters for flapping stiffness and damping changes are small from design study and that is why empirical values are used. The parameters can be changed manually if necessary. The aerodynamic files of fuselage, wings and stabilizers (e.q. horizontal and vertical stabilizers) contain the translation and rotation positioning and the calculated and corrected fuselage polar. Important values like the mass of the fuselage calculated during a flight performance calculation, the position of the center of gravity (C.G.) and the inertia matrix are described in the cell file. The swashplate files describe the dependencies of the command (collective and cyclic control, pedals) to the pitch angles of the rotor blades. The engine model is used to synchronize the rotating directions and speeds of main rotor and anti-torque. It does not represent a dynamic behavior of an engine.

The generation of the flight mechanic model is done automatically by a series of different nested scripts. These scripts need to work correctly with all necessary case discrimination in order to extract the data correctly from the CPACS file and write the corresponding HOST modules without the monitoring of the user.

3.3.   Execution of calculations

To simulate the generated flight mechanic model the trim function of HOST is used in batch mode. The use of time domain simulation in a design process like IRIS is not necessary. To get the important results the trim calculations for unaccelerated stationary flight shows a sufficient accuracy. The most suitable results are required power, forces and moments for different flight conditions. An equilibrium law for the trim considering at least six degrees of freedom has been selected. Here the three translational and three rotational accelerations must be zero. Following a conventional approach the free parameters are four control commands, the collective control, lateral cyclic control, longitudinal cyclic control and yaw control and the two orientations of the fuselage, the pitch and roll angle. Modern configurations like compound or tilt rotorcraft may require even more than six degrees of freedom in order to determine the trim point.

3.3.1   Executing trim calculation and flight speed variation

To setup a specific trim point for computation the target flight condition must be described precisely. This includes information about the flight mass, horizontal and, in case of climb, vertical flight speeds, center of gravity, load factor, altitude and ambient air temperature. In addition the initial values for trim are necessary as start value for the computation.

A typical problem for all higher order simulation tools is the inability to trim a flight condition at higher flight speeds directly after initialization. The initial commands are centered and the values are set to zero as start values because commands can move in a wide range between different flight segment and configurations. Non-linear flow

on the rotor disc may result in strong oscillations of the commands during computation and consequently divergence of the results. Normally the user would manually increase the speed to the desired point and use the previous results as start value for the next computation. To avoid this source of error a variation of the flight speed has been implemented (see FIG 8).

Main part of this procedure is an intelligent control that checks the results and decreases the velocity of the trim point until the computation is performed successfully. Currently the reduction is done in 1 % steps of the end velocity in order to have small steps. The percentage of this reduction is adjustable. Calculations in the batch mode do not store the present results for the next calculation like using the graphical user interface. Therefore the resulting intermediate trim values are stored in a HOST tool specific area of CPACS and updated every time a calculation is performed successfully.

After a successful calculation the velocity is increased. If the calculation is still unsuccessful the velocity is reduced again. As soon as the velocity reaches the target value a final computation of the exact trim point is conducted solving the target flight condition. This procedure is executed every time HOST is used to compute a specific trim point inside a workflow. This can be ether for design mission performance, off-design mission analysis or load case computation.
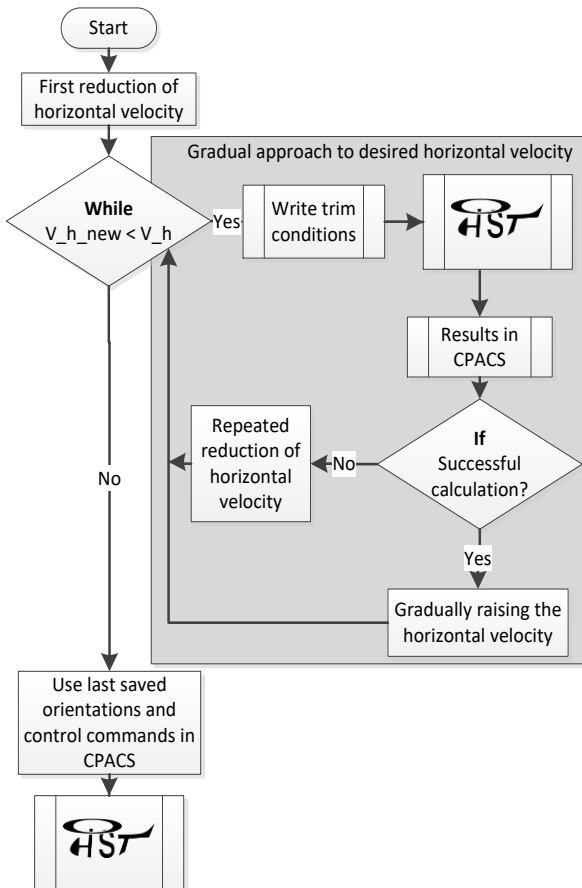

FIG 8   Process for flight speed approach

3.3.2   Mission profile calculation

The core result of the flight performance calculation is the fuel mass estimated for a specific mission profile. For a given design mission the flight mechanic model is trimmed from segment to segment in order to simulate the performance from take-off till landing.

A generic and simple mission profile is shown in FIG 9. It consists of the segments take-off hover, climb, cruise at altitude, descent, landing approach (hover) and an optional reserve. Every segment must have at least two trim points as limits for the integration of the fuel flow.
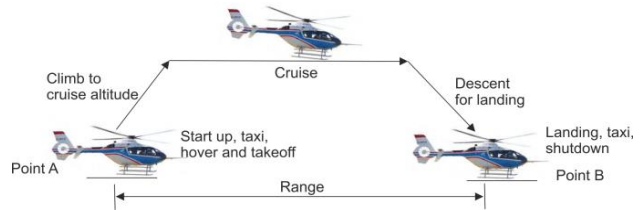

FIG 9   Simple mission profile considering the main flight segments climb, cruise and descent.

If there are long segments (e.g. for a transport mission) a higher number of integration steps per segment are sensible to achieve a sufficient accuracy. For every trim point considered the required power, the control commands and the flight attitude are computed (see chapter 3.3.1). The temporary storage of intermediate results is ensured by the tool specific part of the CPACS data model. To find the correct limits of one integration step the second trim point needs to be interpolated with the fuel flow in order to compute its flight mass due to the initially unknown fuel consumption between the two points. The correct fuel flow for given flight condition (comprising ambient condition and required power) is derived from the engine performance maps scaled in section 2.2.6. The extraction of the fuel flow from the performance maps stored in the CPACS data model is described in section 3.4.

After convergence of the mass of the second point and consequently the average fuel flow for the step the old second point becomes the new first one for the next step. The amount of fuel consumed for every step is summed up for every segment.

Looking top-down there is one loop going through all the flight segments of the given mission. The next loop goes through all steps inside one segment depending on the chosen step length. The following loop iterates the flight mass of the second trim point in one step and therefore computes the fuel consumption. The fourth loop is the intelligent control of the flight speed described in section 3.3.1 ensuring HOST is executed with a reliable solution for the demanded flight condition. In total this highly integrated procedure features four nested loops setting up and executing the trim calculation with HOST for a given mission profile.

Furthermore this complete sub process is conducted for every step in iterating the maximum take-off mass. Consequently the computation of the fuel flow and mission fuel mass is not done on basis of a consistent design with a converged external configuration.

3.4. Extracting engine data and fuel flow

In a first step, the thermodynamic behavior of the engine is represented by pre-calculated performance maps, which consist of a defined set of parameters throughout the entire flight envelope. Performance maps are provided for different ambient conditions and power requirements, whereas the initial model is scaled by air mass flow. Whenever required, these performance maps can be updated and exchanged conveniently within the calculation process.

The interpolation within and between the performance maps is controlled by a separate process. Data storage and interfaces are therefore separated and can be maintained and adapted independently of each other. In the future an extension of the models up to a database of shaft power engines in relevant power classes is conceivable. The interface for data access can be adapted and expanded based on the experience gained in the meantime. A direct coupling of the performance program GTlab with the conceptual helicopter design would also be possible. Finally, the thermodynamic model can be supplemented by further preliminary design processes and the data basis can be extended accordingly by geometric parameters and weight estimates.

3.5. Inverse calculation and mission analysis

Besides the sizing task analyzing off-design missions is an important feature. Hence the possibility of conducting a flight performance computation with an existing model (no matter where it came from) was implemented. For instance the HOST model resulting from sizing can be compared with an existing model from an external source in order to do higher fidelity comparison. In contrast to the flight performance calculation described before (see chapter 3.3.2) the fuel mass is known. The desired results for these computations are either the range with the loaded fuel or the fuel or rather useful mass remaining after completing a mission. Therefore the computation of the two trim points for one integration step has been slightly modified. By now the generic mission profile seen in FIG 9 is implemented for this task. The computation of the fuel consumption follows the description in section 3.4.

3.6. Load case analysis

Part of the higher fidelity analysis (described in section 2.3) is the analysis and design of the structural properties. The necessary input for this task is an analysis of performance requirements considering flight conditions or rather maneuvers outside the design mission. The load cases are calculated by trim calculations. Currently one calculation per load case is executed to calculate a first set up of forces and moments. Even for the dynamic load cases one trim point is considered to get a first idea of the results. In the future more trim points along a load case will be considered to calculate average values for forces and moments to avoid complex time domain simulations in IRIS. The considered load cases are described in the CPACS file. The description consist of different information like flight speed, altitude, fuselage orientation, translational and rotational accelerations for all three axes and the components of the load factor vector n_X, n_Y, n_Z. The total load is given by equation (6).

$$(6) \qquad n = \sqrt{(n_X + n_Y + n_Z)}.$$

The load cases currently taken into account are based on the ADS-33 [21]:

- Hover
- Hovering turn
- Horizontal flight
- Vertical jump
- Banked turn
- Pull down
- Pull up

For every load case a trim condition file will be written and the considered load cases will be processed gradually automated in batch mode. The execution of HOST follows the same procedures as described in chapter 3.3.1. After computing all necessary load cases forces and moments for all components of the HOST model and for all considered flight condition are available. At the end all results are saved in the CPACS file. This first load spectrum of the external forces is the essential input for the dimensioning of the primary structure and it is show to be possible to compute directly after completing sizing.

4. RESULTS

4.1. Design study with variation of main rotor blades and cruise altitude

In order to show the sensitivity of the design process for small adaptions of the virtual configuration three different main rotor blades and two different cruise altitudes are considered. The TLARs listed in TAB 3 are used as input parameter for IRIS. The TLARs are based on the identified parameters for the ACT/FHS (Advanced Control Technology / Flying Helicopter Simulator) research helicopter operated by DLR [22] and also represent a typical civil rescue helicopter. This helicopter is a highly modified variant of an originally EC135. The selected blade geometries for main rotor are a rectangle blade similar to a blade mounted at the BO105, a blade with rounded tip similar to a blade mounted at the ACT/FHS, and an ERATO blade.

TAB 3   TLARs related to ACT/FHS and representing a contemporary rescue helicopter

Minimum Parameter	Value
Payload mass, kg	809
Cruise speed, m/s	65
Range, km	615
Number of main rotor blades	4
Main rotor arrangement	Standard
Optional Parameter	
Blade geometry (Main rotor)	Rectangle, Rounded tip, ERATO
Mission profile	Standard
Cabin length, m	1.7
Cabin width, m	1.5
Cabin height, m	1.25
Cruise altitude, m	1000, 2000

The procedure follows the description in section 2.2. Also different cruise altitudes with 1000 m and 2000 m are considered. The mission profile is a simple standard profile shown in FIG 9.

In FIG 10 the 3D output of IRIS shows the results for the three different configurations using different main rotor blades.

The basic results of IRIS for 1000 m cruise altitude are shown in TAB 4. By variation of the main rotor blade the resulting take-off mass changed for a constant cruise altitude. Starting with 2806 kg using a rectangle blade, the take-off mass drops to 2755 kg with a ERATO blade. Major influence on the maximum take-off mass has the calculated fuel mass. The configuration using an ERATO blade needs 39 kg less fuel mass then equipped with a rectangular blade due to the more sensible blade geometry and airfoils for cruise conditions. Small changes in radius, mean chord and rotating speed are necessary during the sizing loop to compensate for different maximum take-off masses.
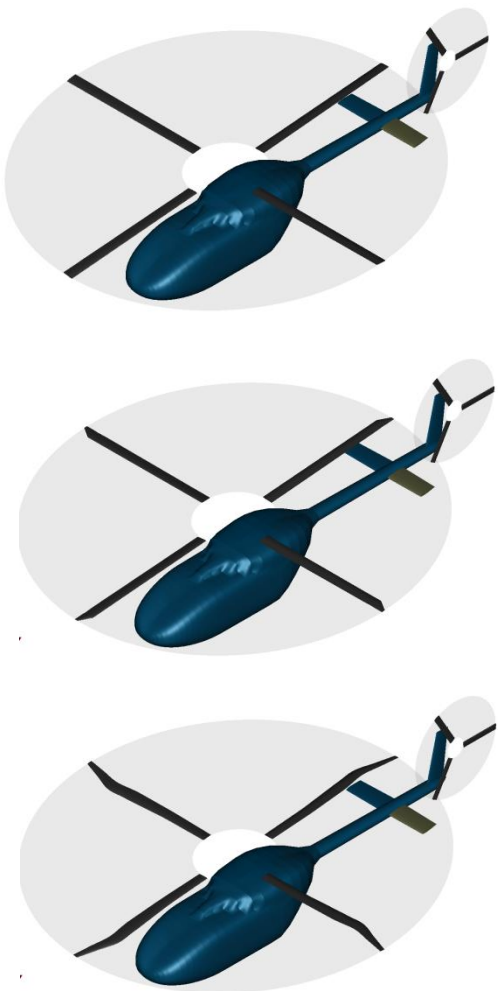
TAB 4   Selected results of IRIS for 1000 m cruise altitude

Parameter	Rectangle blade	Rounded tip blade	ERATO-blade
m_{MTOM}, kg	2806	2787	2755
m_{BEM}, kg	1547	1543	1535
m_F, kg	450	435	411
R_{MR}, m	5.069	5.058	5.039
c_{MR}, m	0.276	0.275	0.273
Ω_{MR}, rad/s	41.42	41.52	41.68

Another comparison is shown in TAB 5 by increasing the cruise altitude from 1000 m to 2000 m.

TAB 5   Selected results of IRIS for 2000 m cruise altitude

Parameter	Rectangle blade	Rounded tip blade	ERATO
m_{MTOM}, kg	2776	2753	2739
m_{BEM}, kg	1543	1537	1535
m_F, kg	424	407	394
R_{MR}, m	5.054	5.039	5.039
c_{MR}, m	0.275	0.273	0.273
Ω_{MR}, rad/s	41.55	41.68	41.68

Fuel consumption slightly diminishes due to the reduced parasite drag at higher altitude. Here the ambient conditions are not only taken into account by the trim calculations but also by the thermodynamic engine model. The maximum take-off mass for the configurations from 1000 m to 2000 m cruise altitude shows a deviation up to - 1.2 %. The calculated fuel mass for the required range of 615 km at 2000 m cruise altitude compared to 1000 m cruise altitude shows a deviation up to - 6.4 %.

Plots of the flight mass (black) and fuel flow (red) along the generic mission profile is plotted over the iteration steps shown in FIG 11 for 1000 m cruise altitude. The highest fuel flow occurs at climb phase because of the highest necessary power during this phase to compensate the take-off mass while working against the gravity. The lowest fuel flow is calculated for the descent. During the cruise phase the fuel flow is almost constant for one configuration. The configuration using the ERATO blade shows the lowest fuel flow during cruise phase. The highest fuel flow during the mission profile is shown by the configuration with a simple rectangular blade.

Furthermore the progress of the flight mass during the cruise phase can be seen in FIG 11. During this flight time the diminishment of flight mass due to the fuel consumption is nearly linear. The total fuel mass during descent is rather small.

FIG 10 3D geometry outputs of IRIS for a standard configuration using a rectangle blade (top), rounded tip (mid) and a ERATO blade (bottom)
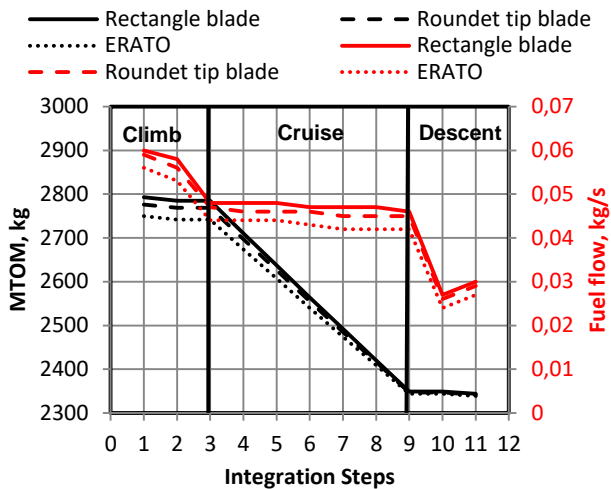
FIG 11 Behavior of take of mass (black) and fuel flow (red) along a simple mission profile for different used main rotor blades for 1000 m cruise altitude

4.2. Comprehensive analysis of the generated flight models

The resulting configurations with their corresponding HOST models after the sizing loop are now analyzed in more detail like described in chapter 3.5. The configurations generated during the sizing process (chapter 4.1) can be directly compare with the reference HOST model of the ACT/FHS for a specified take-off mass of 2910 kg and a fuel mass of 560 kg.

The results for range, with given fuel mass, at different flight speeds, for the different configurations compared to the ACT/FHS reference model is shown in FIG 12.

The flight speed ranges from 5 m/s to 60 m/s. All configurations use the exactly same take-off mass, fuel mass and engine scaling. Hence the presented differences are only related to the different flight mechanical models.

Obviously the larger the speed, required power and fuel consumption the larger the differences in possible range are.

During the highest calculated flight speed 60 m/s at MSL (Main See Level) the configurations present the lowest possible ranges around 700 km. The best resulting range can be seen at a cruise altitude of 2000 m with ranges between 800 km up to 900 km for the configuration using an ERATO blade. Generally it can be seen that the ERATO blade configuration shows the best performance for all calculated cruise altitudes. Between the ACT/FHS model and the configurations using a blade with rounded tip similar to the ACT/FHS blade an offset for all three cruise altitudes is displayed. Because of the tables for the fuselage aerodynamics differ, despite the assumed fuselage dimensions of the reference helicopter ACT/FHS, the fuselage of the virtual and reference flight mechanical model are not identical. To justify the difference, the coefficients do not take all irregularities of the fuselage into account. This effect is clearly visible at higher flight speeds.
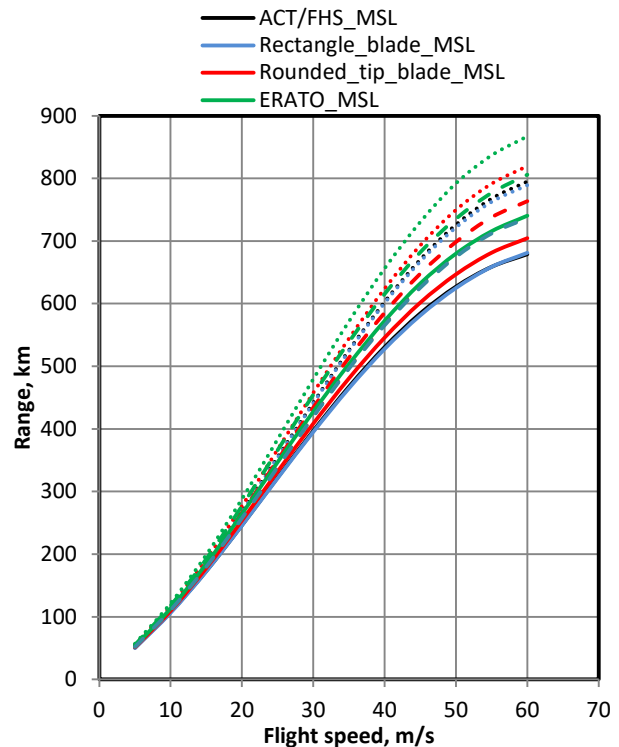

FIG 12 Range vs. flight speed for the reference helicopter ACT/FHS (black), configuration with a rectangle blade (blue), configuration with a rounded tip (red) and a configuration with a ERATO blade (green) at different cruise altitudes: MSL (solid lines), 1000 m (dashed lines) and 2000 m (dotted lines)

A comparison of the fuel flow during a variation of the flight speed is shown in FIG 13 for the reference and the three virtual configurations. Here two different take-off masses are considered.

The two used masses are the maximum take-off mass of the ACT/FHS 2910 kg and a lighter mass of 2200 kg using a fewer payload. The results show generally the lowest fuel flow during the cruise speed between 30 and 40 m/s. This can be determined as the best operating point for the used engine model.

Besides the general offset between the results for the two different take-off masses the necessary fuel flow during hover for the heavy variant is significant higher because of the higher required power during this phase. Similar to FIG 12 the configuration with an ERATO blade shows the best behavior for fuel flow. The ACT/FHS reference configuration and the configuration using a rounded tip show an offset at with increasing flight speed due to differences in parasite drag discussed earlier. The configuration using a rectangular blade shows the highest fuel flow. Since the induced power diminishes at higher flight speeds it is at maximum in hover. The parasite power is independent of the flight mass, neglecting a change in angle of attack due to the change in the trim angles. The curves for different flight masses get closer to each other at higher speeds. The fuel flow in hover drops below the consumption at high speed cruise for all lighter configurations.
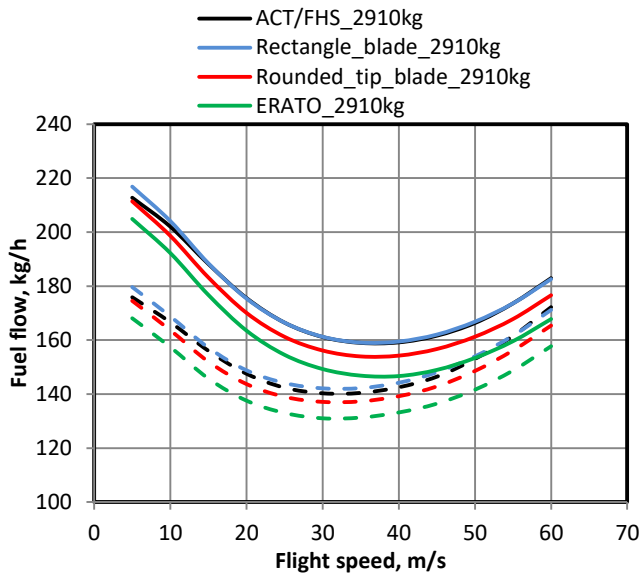
FIG 13 Fuel flow vs. flight speed for the reference helicopter ACT/FHS (black), configuration with a rectangular blade (blue), configuration with a rounded tip (red) and a configuration with a ERATO blade (green) for different take-off masses: 2910 kg (solid lines) and 2200 kg (dashed lines)

4.3. Load case analysis

The sections 2.3 and 3.6 already mentioned the use of HOST integrated into the design environment to compute load cases for structural analysis and design. The calculated results of forces and moments at the significant components are applied as external forces for the modelling of a finite element analysis. To show first results of the possible load case analysis in batch mode the generated HOST model of the configuration using a rectangle blade (see top FIG 10) was used. Forces and moments can be computed from HOST for fuselage, vertical stabilizer, horizontal stabilizer, main rotor and tail rotor. Because of the many results only the forces for four selected components are shown in FIG 14. The load cases considered in this demonstration are a selection of those listed in chapter 3.6. For all load cases the force at main rotor in Z-coordinate shows the highest value to compensate the flight mass which is affected by the appearing gravity.

The force on the main rotor along x axis shows the highest values during horizontal flight and banked turn. During hover case the x force shows the lowest value because of no velocity and acceleration acting on the helicopter. The highest force value on the fuselage along x axis is acting during the horizontal flight because of the fast forward velocity. The vertical and horizontal stabilizers only have an effect during forward movement of the helicopter. Therefore during hover and hovering turn the aerodynamic areas show no effect. The highest value is calculated during horizontal flight.
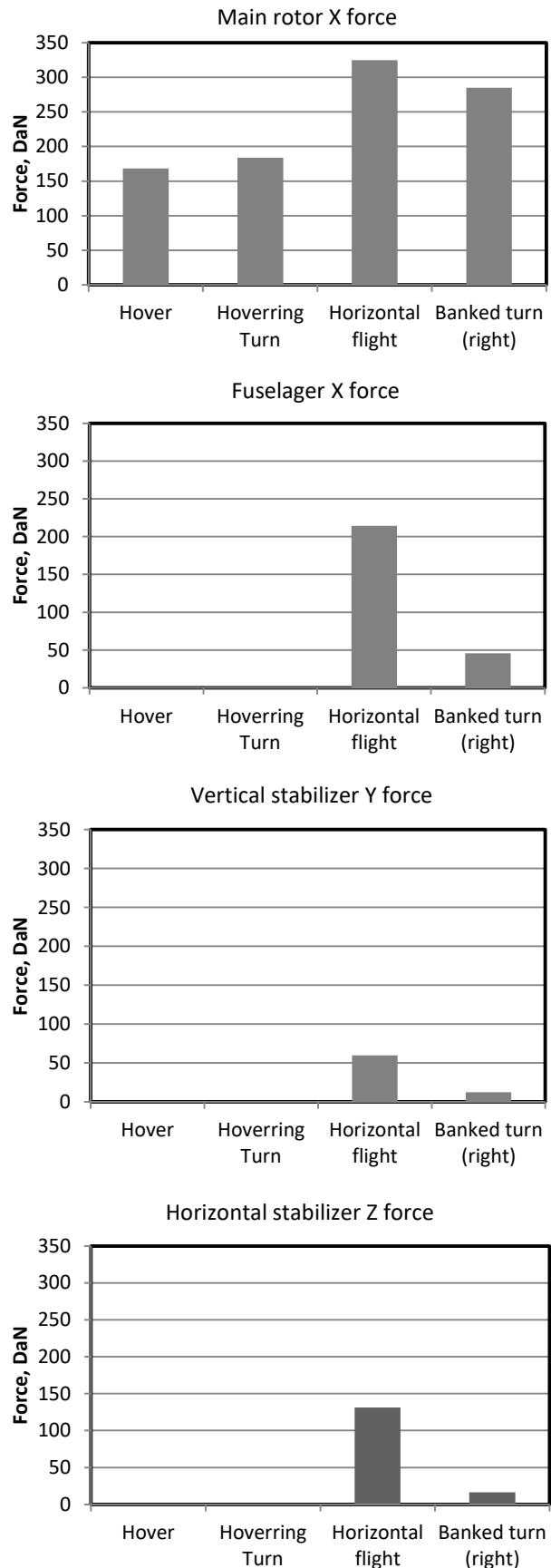

FIG 14 Comparison of resulting forces for a standard configuration with rectangle main rotor blade

5. SUMMARY

5.1. Conclusions

This paper presented an overview of the rotorcraft design workflow IRIS and the implementation of the flight simulation tool. Focus was on the calculations during the sizing process of IRIS and the implementation and necessary automatization of the procedures connected with HOST.

The flight performance calculations applying HOST was coupled with a thermodynamic engine model inside the sizing process to calculate the fuel consumption at all flight conditions along the design mission.

Furthermore the use of this approach in a comprehensive analysis for off-design missions is also presented by an inverse flight performance calculation analyzing the useful mass for a determined mission.

The algorithms to compute flight conditions for mission analysis are further used to compute load cases for a following structural analysis.

The benefit of implementing such a complex flight simulation tool like HOST into the sizing task of IRIS is to enable an easy feedback of information from comprehensive analysis for targeted optimization.

5.2. Outlook

Since this approach is by now the most accurate and still possible computation inside a design loop the focus is now on increasing the accuracy of the model.

An efficient and accurate computation of the aerodynamics is still major part of the ongoing research. This will also include lifting surfaces and stabilizers with control surfaces.

The principle of a modular design system is now in development following the guidelines already demonstrated by applying different reference blades. The goal is to increase the diversity of the design cases without increasing uncertainties. The future configuration will include case studies for high speed compound rotorcraft as well as multi rotor configurations for urban air mobility.

REFERENCES

[1] P. Weiand, M. Buchwald and D. Schwinn, "Process Development for Integrated and Distributed Rotorcraft Design," *MDPI Journal,* pp. Volume 6, Issue 2, 2019.

[2] D. Raymer, "Aircraft Design: A Conceptual Approach," American Institute of Aeronautics and Astronautics, Reston, VA, 2006.

[3] J. Roskam, Airplane Design, Airplane Cost Estimation: Design, Development, Manufacturing and Operating, Lawrence, Kansas, USA: Design, Analysis and Research Corporation, 2018.

[4] P.-M. Basset, A. Tremolet, F. Cuzieux, C. Schulte, D. Tristrant, T. Lefebvre, G. Reboul, M. Costes, F. Richez, S. Burguburu, D. Petot and B. Paluch, "The C.R.E.A.T.I.O.N. project for rotorcraft conepts evaluation: The first steps," in *37th European Rotorcraft Forum*, Vergiate and Gallarate, Italy, 2011.

[5] P.-M. Basset, A. Tremolet, F. Cuzieux, G. Reboul, M. Costes, D. Tristrant and D. Petot, "C.R.E.A.T.I.O.N. the ONERA Multi-Level Rotorcraft Concepts Evaluation Tool: The Foundations," in *Future Vertical Lift Aircraft Design Conference*, San Francisco, CA, 2012.

[6] W. Johnson, "NDARC: NASA Design and Analysis of Rotorcraft," NASA/TP-2009-215402, 2009.

[7] W. Johnson, "CAMRAD II Software Description," [Online]. Available: http://www.johnson-aeronautics.com/documents/CAMRADIIoutline.pdf. [Accessed 29 06 2018].

[8] P. M. Basset, P. Beaumier and T. Rakotomamonjy, "C.R.E.A.T.I.O.N.: A numerical workshop for rotorcraft concepts generation and evaluation," in *Rotorcraft Virtual Engineering Conference*, Liverpool, UK, 2016.

[9] B. Boden and R. Mischke, "Entwicklung der Forschungssoftware RCE," in *Free and Open Source Software Conference*, Sankt Augustin, Germany, 2018.

[10] DLR, "RCE environment," [Online]. Available: https://rcenvironment.de/. [Accessed 23 05 2019].

[11] J. Jepsen, P.-D. Ciampa, B. Nagel and V. Gollnick, "Design of a common library to simplify the implementation of aircraft studies in CPACS," in *Deutscher Luft- und Raumfahrtkongress*, Hamburg, Germany, 2015.

[12] B. G. van der Wall, C. Kessler, Y. Delrieux, P. Beaumier, M. Gervais, J.-F. Hirsch, K. Pengel, P. Crozier, "From Aeroacoustics Basic Research to a Modern Low-Noise Rotor Blade," *Journal of the American Helicopter Society,* vol. 62, no. 4, pp. 1-16, 2017.

[13] D. Schwamborn, T. Gerhold und R. Kessler, „The DLR-Tau Code: an Overview," in *ONERA - DLR Aerospace Symposium*, Paris, France, 1999.

[14] P. Kunze, "Parametric Fuselage Geometry Generation and Aerodynamic Performance Prediction in Preliminary Rotorcraft Design," in *39th European Rotorcraft Forum*, Moscow, Russia, 2013.

[15] C. N. Keys and R. Wiesner, "Guidelines for Reducing Helicopter Parasite Drag," *Journal of the American Helicopter Society,* vol. 20, no. 1, pp. 31-40, 1975.

[16] D. Oliver, Jane's Helicopter Markets and Systems, Surrey, UK: Janes's, 2009.

[17] R. G. Becker, F. Wolters, N. Nauroz and T. Otten, "Development of a gas turbine performance code and its application to preliminary engine design," in *Deutscher Luft- und Raumfahrtkongress*, Bremen, Germany, 2011.

[18] D. Schwinn, P. Weiand, M. Schmid und M. Buchwald, „Structural sizing of a rotorcraft fuselage using an integrated design approach," in *31th Congress of the International Council of the Aeronautical Sciences*, Belo Horizonte, Brazil, 2018.

[19] B. Benoit, A.-M. Dequin, K. Kampa, W. von Grünhagen, P.-M. Basset, B. Gimonet, "HOST, a General Helicopter Simulation Tool for Germany and France," in *American Helicopter Society 56th Annual Forum*, Virginia Beach, VA, 2000.

[20] M. Buchwald, P. Weiand, D. Schwinn and M. Schmid, "Flight performance calculation of rotorcraft in the conceptual design phase," in *Deutscher Luft- und Raumfahrtkongress*, Friedrichshafen, Germany, 2018.

[21] U. S. Army, "Aeronautical Deign Standard Performance Specification Handling Qualities Requirements For Military Rotorcraft," Alabama, USA, 2000.

[22] J. Kaletka, H. Kurscheid and U. Butter, "FHS: the New Research Helicopter: Ready for Service," *Aerospace Science and Technology,* vol. 9, no. 5, pp. 456-467, 2005.

[23] W. Johnson, C. Silva and E. Solis, "Concept Vehicles for VTOL Air Taxi Operations," in *Aeromechanics Design for Transformative Vertical Flight 2018*, San Francisco, 2018.